Crystal Lattice Effects on the Electronic Spectrum of the Manganate Ion

By **Peter Day**, University of Oxford, Inorganic Chemistry Laboratory, South Parks Road, Oxford
Lorenzo DiSipio, Laboratorio di Chimica e Tecnologie dei Radioelementi del C.N.R., Padova, Italy
Giulio Ingletto and **Luigi Oleari**, Università di Parma, Istituto di Chimica Fisica, Parma, Italy

The polarised electronic spectra of MnO_4^{2-} doped into crystals of Rb_2SO_4, Cs_2SO_4, and K_2CrO_4 have been recorded at 4·2 K in the range 10 000—40 000 cm^{-1}. The different polarisation behaviour of the low-symmetry components of the $^2T_2$ terms derived from the ligand-field and charge-transfer configurations is ascribed to differences in the magnitude of the spin-orbit interaction in the two types of configuration. From an analysis of the phonon sidebands in the ligand-field spectrum, comments are made about the phonon spectra of the host lattices. Shifts in the ligand-field and charge-transfer origins on changing the host lattice are also discussed.

In a recent paper [1] we examined the electronic spectrum of the $3d^1$ tetra-oxo-ion MnO_4^{2-}, doped into a crystal of K_2SO_4. From the linearly polarised spectra recorded at 4·2 K we were able to make precise assignments of the ligand-field and the first four charge-transfer transitions. The transitions which are all of $^2T_1$ or $^2T_2$ parentage, are split by the field of the C_s site in the K_2SO_4 lattice into three components. In the case of the ligand-field band and the first charge-transfer band, all three components are clearly resolved, and the polarisations of the zero-phonon lines demonstrate that the charge-transfer band is of $^2T_2$ parentage. In the C_s site a $^2T_2$ term becomes $2^2A' + {}^2A''$, the former allowed from the $^2E_{x^2-y^2}$ ground state when the electric vector is polarised along the b-axis and the latter when it is polarised along a or c. In fact we found that the first charge-transfer transition has two zero-phonon lines in the $E \parallel b$ spectrum and one in the $E \parallel a$. On the other hand the ligand-field transition, which must also perforce be of $^2T_2$ parentage, has three zero-phonon lines, but all are present in both the

[1] L. DiSipio, L. Oleari, and P. Day, *J.C.S. Faraday II*, 1972, **68**, 776.

$E \parallel b$ and $E \parallel a$ spectra. We anticipated that this curious behaviour was the result of an interplay between lattice induced distortion of the MnO_4^{2-} ion and spin-orbit coupling in the Mn 3*d* shell. It therefore appeared worthwhile to examine the effect on the MnO_4^{2-} spectrum of changing the host crystal. Furthermore, one notable feature of the MnO_4^{2-} ligand-field transition in the K_2SO_4 lattice was the wealth of phonon sideband structure due to coexcitation not only of intramolecular, but also lattice modes. The degree of resolution of the electronic spectrum is such that it may prove possible to use it to estimate the density-of-states curves of the various phonon branches, a procedure which has yielded interesting results for transition-metal ions doped in continuous oxide lattices [2] and for organic molecular crystals,[3] but which has never to our knowledge been applied to inorganic molecular ionic solids. For this reason we have chosen a set of isostructural host crystals in which the mass of the cation is varied while that of the anion remains constant (K_2SO_4, Rb_2SO_4, Cs_2SO_4) and have also varied the mass of the anion (K_2SO_4 and K_2CrO_4). Another point of interest is the possibility of observing the effect both on ligand-field and charge-transfer states of varying the Madelung potential surrounding the ion.

EXPERIMENTAL

Crystals were grown by slowly evaporating aqueous 10M-KOH solutions of the appropriate alkali-metal sulphate or chromate, containing a small concentration of K_2MnO_4. The orientation of the crystal axes was determined from the external morphology,[4] checked in a number of cases by Weissenberg photographs.

The spectra were recorded using Cary 14 spectrophotometers, both in Oxford and Parma. The Oxford spectrophotometer employs an Oxford Instruments CF 100 continuous-flow helium cryostat, while that in Parma uses a static-liquid helium cryostat of conventional design. In both cases the incident light was polarised by a calcite Glan prism. Spectra of all the crystals were measured with the electric vector polarised along the *a* and *b* crystallographic axes.

Description of the Spectra

The Charge-transfer Bands.—The polarised spectra of MnO_4^{2-} in the three lattices Rb_2SO_4, Cs_2SO_4, and K_2CrO_4 are shown in Figures 2, 4, and 6, and the frequencies of the peak maxima are collected in Tables 1 and 2.

In the K_2CrO_4 host only the lowest-energy charge-transfer band of MnO_4^{2-} is visible, the higher ones being obscured by the charge-transfer absorption of the chromate.

In all four host lattices the lowest-energy charge-transfer band shows well resolved vibrational fine structure, so that the peak positions can be estimated to *ca.* ± 10 cm^{-1}. The structure of the higher-energy bands is broadened out, however, and for these we can only locate the peaks and shoulders to *ca.* ± 50 cm^{-1}. Consequently for bands other than the lowest our assignments of the peaks to particular vibrational excitations cannot be very precise. The frequencies of the internal modes of MnO_4^{2-}, required for the assignment of the vibronic fine structure in our spectra, have only been reported for the potassium salt; [5] they are: $\nu_1(a_1)$ 810 cm^{-1}, $\nu_3(t_2)$ 843 and 869 cm^{-1} and $\nu_4(t_2)$ 328 cm^{-1}. By comparison with other tetra-oxo-ions $\nu_2(e)$ should lie close to ν_4, possibly a little lower. With these frequencies the assignment of the fine-structure of the charge-transfer spectrum in the three new host lattices follows by analogy with the assignment already reported for the K_2SO_4 host

TABLE 1

Frequencies of the vibronic components of the first charge-transfer band of MnO_4^{2-} in different host lattices (cm^{-1})

(*a*) $E \parallel b$ spectrum

Rb_2SO_4	Cs_2SO_4	K_2CrO_4	Assignment
16 097	15 998	15 845	IA
16 171	16 053	16 019	IB
16 431	16 301		IA + ν_4
	16 357		IB + ν_4
16 857	16 759	16 642	IA + ν_1
16 976	16 817	16 790	IB + ν_1
17 183	17 063		IA + ν_1 + ν_4
	17 124		IB + ν_1 + ν_4
17 642	17 521	17 414	IA + $2\nu_1$
17 776	17 585	17 589	IB + $2\nu_1$
17 982	17 822		IA + $2\nu_1$ + ν_4
	17 876		IB + $2\nu_1$ + ν_4
18 403	18 285	18 172	IA + $3\nu_1$
18 488	18 349		IB + $3\nu_1$
18 748			IA + $3\nu_1$ + ν_4
	18 627		IB + $3\nu_1$ + ν_4
	19 032	18 868	IA + $4\nu_1$
(19 231)			IB + $4\nu_1$
(19 950)	(19 802)	19 631	IA + $5\nu_1$
		20 420	IA + $6\nu_1$

(*b*) $E \parallel a$ spectrum

16 235	16 125	16 015	IC
16 313	16 244	16 160	IC + ν_L
16 511	16 417	16 272	IC + ν_4
17 020	16 894	16 770	IC + ν_1
17 094	17 017	16 923	IC + ν_1 + ν_L
17 289	17 180	17 021	IC + ν_1 + ν_4
17 785	17 671	17 544	IC + $2\nu_1$
17 885	17 774	17 690	IC + $2\nu_1$ + ν_L
18 054	17 947	17 801	IC + $2\nu_1$ + ν_4
18 569	18 413	18 290	IC + $3\nu_1$
18 658	18 519	18 445	IC + $3\nu_1$ + ν_L
18 834	18 723	18 559	IC + $3\nu_1$ + ν_4
19 343	19 214	19 032	IC + $4\nu_1$
19 434			IC + $4\nu_1$ + ν_L
19 602	19 451	19 329	IC + $4\nu_1$ + ν_4
(20 092)	19 952	(19 767)	IC + $5\nu_1$
(20 205)			IC + $5\nu_1$ + ν_L
(20 408)	20 250, 20 249	(20 082), 20 025	IC + $5\nu_1$ + ν_4

Calculated frequencies and origins:

(*a*) $E \parallel b$ spectrum:

	K_2SO_4	Rb_2SO_4	Cs_2SO_4	K_2CrO_4
IA	16 129	16 097	15 998	15 845
IB	16 245	16 171	16 053	16 019
ν_1	792	778	762	774
ν_4	320	322	303	

(*b*) $E \parallel a$ spectrum:

IC	16 313	16 235	16 125	16 015
ν_1	785	778	766	750
ν_4	280	266	292	260
ν_L	122	85	114	150

[2] L. E. Ralph and M. G. Townsend, *J. Phys.*, 1970, *C*, **3**, 8.
[3] See, *e.g.*, 'Excitons, Magnons and Phonons in Molecular Crystals,' ed. A. B. Zahlan, Cambridge University Press, 1968.
[4] P. Groth, Chemisches Krystallographie, Leipzig, 1908.
[5] W. P. Griffith, *J. Chem. Soc.* (*A*), 1966, 1467.

lattice. The fine-structure accompanying the first charge-transfer band in both $E \parallel a$ and $E \parallel b$ spectra is sufficiently sharp that we have thought it worth computing average values of the excited state vibrational frequencies. For the higher charge-transfer bands this is not worthwhile.

resolved spectrum is that in Cs_2SO_4, and the worst, K_2CrO_4. In the latter, it is quite difficult to discern the two origins in the $E \parallel b$ spectrum because the higher-energy one appears only as a shoulder.

As with the lowest-energy charge-transfer band, the

TABLE 2

Frequencies of the higher energy charge-transfer bands of MnO_4^{2-} in different host lattices (cm^{-1})

K_2SO_4		RB_2SO_4		Cs_2SO_4		
$E \parallel a$	$E \parallel b$	$E \parallel a$	$E \parallel b$	$E \parallel a$	$E \parallel b$	
(22 220)	(22 222)	(22 124)	(22 272)	(22 148)	(22 222)	II
(23 095)	23 136	(23 095)	23 229	(22 936)	23 015	
23 697				23 529	23 725	
	23 848	23 781	23 793			
23 981						
(24 390)	24 450	24 361	24 450	24 213	24 390	
	25 506	(25 316)	25 349	25 157	25 126	
26 600	26 316	(26 560)	26 192	(25 940)	(25 974)	III
				(26 178)	(26 137)	III + ν_4
27 322	27 178	(27 397)	(27 027)	26 702		III + ν_1
				26 936	26 954	III + ν_1 + ν_4
	28 076	28 011	27 855	(27 473)		III + $2\nu_1$
				27 778	27 755	
		28 612		(28 571)	28 751	
29 455	(29 412)	29 180	29 197	29 028		IV
				29 586	29 326	
30 211	30 009	29 958	30 030		30 030	IV + ν_1
30 960	30 853	30 600	30 600	(30 395)	(30 675)	IV + $2\nu_1$
		(30 817				
31 686		(31 447)		31 056		IV + $3\nu_1$
32 362				31 766		IV + $4\nu_1$
		(32 206)	(32 573)	(32 468)	32 000	V
33 278	(33 797)	(33 025)	32 916	(33 058)	32 787	V + ν_1
33 956	34 483	(33 750)	33 467	33 481	33 445	V + $2\nu_1$
34 602	35 034	34 364		34 662	34 130	V + $3\nu_1$
35 273	35 564	35 026	35 336		34 813	V + $4\nu_1$
36 036	36 364	(35 714)	36 036		35 486	V + $5\nu_1$
	37 120		36 724		36 153	V + $6\nu_1$
					37 010	V + $7\nu_1$

In all four host lattices, the first charge-transfer band is built on three origins, two in the $E \parallel b$ spectrum and one in

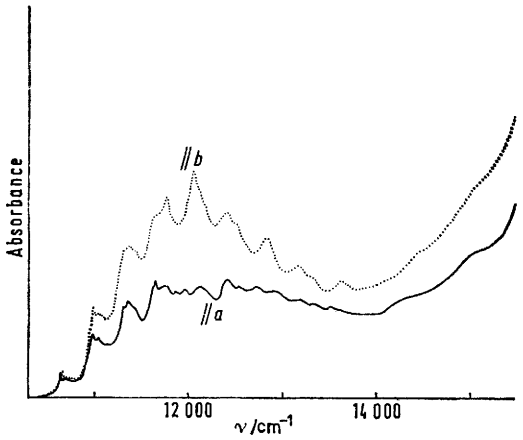

FIGURE 1 The ligand-field spectrum of MnO_4^{2-} in Rb_2SO_4 at 4·2 K

the $E \parallel a$. These are labelled IA, IB, IC in Table 1. Accompanying each is a long progression in ν_1, each member of which shows weaker co-excitation of ν_4 (or possibly ν_2) and, in the $E \parallel a$ spectrum only, an additional lower-frequency excitation which we assign to a lattice mode. The best

higher ones are best resolved in Cs_2SO_4. There are also some variations in the relative intensities of the various transitions on changing the host lattice, several of which serve to confirm the assignments of particular regions of absorption to separate electronic transitions which we had already tentatively made from the spectrum in the K_2SO_4 host lattice alone. For example, in the K_2SO_4 spectrum two bands are seen in the $E \parallel b$ polarisation at 26 316 and

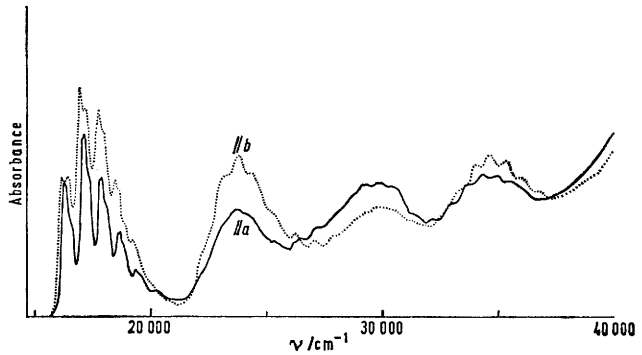

FIGURE 2 The charge-transfer spectrum of MnO_4^{2-} in Rb_2SO_4 at 4·2 K

27 178 cm^{-1} which appear to form part of a new band system separate from the more intense ones on either side. In both

the Rb_2SO_4 and Cs_2SO_4 spectra this region is much better resolved, and particularly in the latter, reveals the beginnings of a substantial progression. The relative intensities of each band system in different polarisations do not vary very much from one host lattice to another, though.

The Ligand-field Band.—The polarised spectrum of MnO_4^{2-} in the ligand-field region is shown in Figures 1, 3, and 5 and the band frequencies are listed in Table 3.

spectra in the three sulphate lattices and that in the chromate. No doubt this is due to the similarity between the masses of CrO_4^{2-} and MnO_4^{2-}, and hence to the stronger coupling between the electronic excitation of the guest and the lattice modes of the host. It is also of interest to note that underlying the sharp line structure in all four spectra there appears to be a broad and rising continuum of absorption. It may be that it is simply the result of overlapping

TABLE 3

Frequencies of the vibronic sidebands of the ligand-field transition of MnO_4^{2-} in different host lattices (cm^{-1})

Rb_2SO_4		Cs_2SO_4		K_2CrO_4		
E // *a*	*E* // *b*	*E* // *a*	*E* // *b*	*E* // *a*	*E* // *b*	
10 721	10 723	10 553	10 556	10 646	10 647	I
10 789	10 790	10 612	10 612	(10 695)	(10 697)	I + ν_L (1)
		10 662	10 656			I + ν_L (2)
10 843	10 857	10 685	10 687	(10 735)	(10 741)	I + ν_L (3)
		10 854	10 824	(10 905)	(10 893)	I + ν_4
11 062	11 064	10 890	10 890	10 975	10 975	II
11 134	11 131	10 949	10 948	11 041	11 034	II + ν_L (1)
		10 994	11 000			II + ν_L (2)
11 183	11 188	11 020	11 023		11 077	II + ν_L (3)
		11 078	11 091	11 142	(11 152)	II + ν_L (4)
		11 174	11 157			II + ν_4
11 400	11 392	11 217	11 213	11 308	11 315	III
				11 354	11 351	III + ν_L (1)
		11 312	11 261			III + ν_L (2)
11 497	11 509	11 334	11 330			III + ν_L (3)
				(11 419)	11 417	I + ν_1
11 696	11 710	11 486		11 628	11 655	III + ν_4
		11 522	11 514	11 662		
		11 459				
11 851	11 847	11 667	11 656	11 751	11 756	II + ν_1
11 952	11 981	11 785	11 789	11 860	11 834	II + ν_1 + ν_L (3)
		11 855	11 869	11 955	11 957	II + ν_1 + ν_L (4)
		11 954				II + ν_1 + ν_4
12 180	12 178	11 991	11 983	12 114	12 066	III + ν_1
12 272	12 250					III + ν_1 + ν_L (1)
		12 105	12 105	(12 195)	12 183	III + ν_1 + ν_L (3)
		12 195				III + ν_1 + ν_L (4)
12 483	12 500	12 258	12 294	12 429	12 407	III + ν_1 + ν_4
		12 321				
12 612	12 625	12 438	12 425	12 539	12 508	II + $2\nu_1$
12 760	12 780	12 553	12 558			II + $2\nu_1$ + ν_L (3)
		12 646	12 637	12 739		II + $2\nu_1$ + ν_L (4)
12 961	12 965	12 758	12 754	12 828	12 837	III + $2\nu_1$
13 098	13 100	12 879	12 873			III + $2\nu_1$ + ν_L (3)
13 255	13 275	13 090	13 050	(13 210)	13 172	III + $2\nu_1$ + ν_4
13 408	13 402	13 181	13 188	(13 298)	13 298	II + $3\nu_1$
		13 307				II + $3\nu_1$ + ν_L (3)
13 750	13 739	13 530	13 518			III + $3\nu_1$
	13 867	13 642				III + $3\nu_1$ + ν_L (3)
	14 074					III + $3\nu_1$ + ν_4
14 205	14 180	13 932	13 937			II + $4\nu_1$
14 519	14 513		14 310			III + $4\nu_1$
	14 855					III + $4\nu_1$ + ν_4
	15 071					II + $5\nu_1$
	15 307					III + $5\nu_1$

Table 3 displays the relationship between the origins and vibronic sidebands in the different hosts, and though there may be some ambiguity about a few weaker, more diffuse features in the higher frequency parts of the band systems, the correlation between the major groups of peaks is quite clear.

To an even greater extent than in K_2SO_4, the ligand-field spectra of MnO_4^{2-} in Rb_2SO_4, Cs_2SO_4, and K_2CrO_4 reveal a wealth of fine structure. The best resolved spectrum is that in Cs_2SO_4, and there are interesting differences between the between increasingly diffuse bands, or that the baseline is being affected by scattering of light from defects in the crystals. However, no such effect is observed, for example, in the first charge-transfer band, so we are inclined to think that it is real. It could be significant that a similar continuum absorption accompanies the sharp-line structure of the weak near-infrared $^1T_1$ transition in MnO_4^-.[6,7] In every case the *E* // *b* spectrum is more intense throughout the whole band system than the *E* // *a*.

The band systems in all four lattices are assignable to three

[6] P. Day, L. DiSipio, and L. Oleari, *Chem. Phys. Letters*, 1970, **5**, 533.

[7] J. C. Collingwood, P. Day, R. G. Denning, D. Robbins, L. DiSipio, and L. Oleari, *Chem. Phys. Letters*, 1972, **13**, 567.

electronic origins, all of which appear in both polarisations. Built on these origins are progressions in up to five quanta of

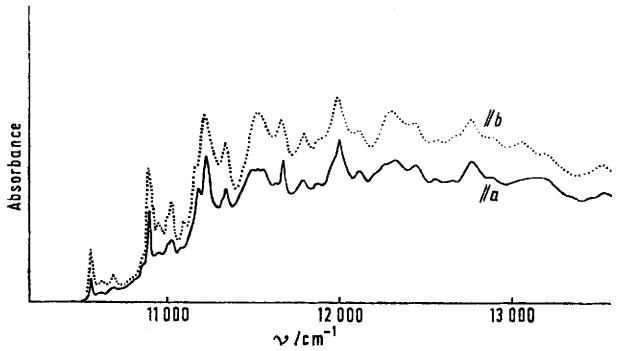

FIGURE 3 The ligand-field spectrum of MnO_4^{2-} in Cs_2SO_4 at 4·2 K

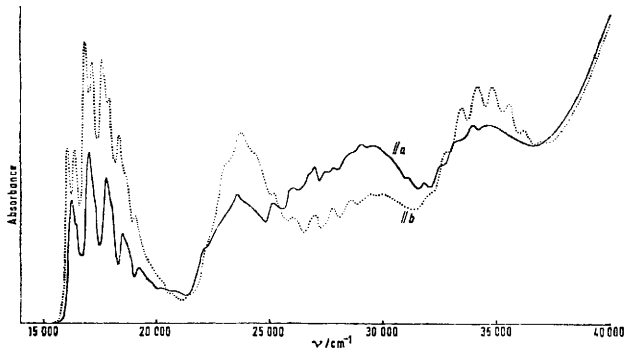

FIGURE 4 The charge-transfer spectrum of MnO_4^{2-} in Cs_2SO_4 at 4·2 K

ν_1, together with weaker excitations of single quanta of non-totally symmetric modes. The frequency intervals along the major progressions show little evidence of anharmonicity. The low-frequency vibrational intervals, which we assign to lattice modes, are better resolved than in the first charge-transfer band, and in the Cs_2SO_4 lattice, four sets of intervals are discernible. In the other lattices, fewer are seen, but Table 3 correlates the lattice vibrational intervals between the various compounds.

In assigning the sidebands due to lattice modes we are handicapped by the scarcity of precise vibrational data on the alkali-metal sulphates. No single-crystal Raman studies appear to have been carried out, other than on Na_2SO_4,[8]

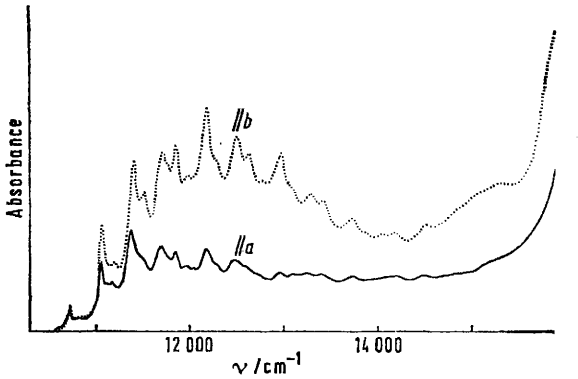

FIGURE 5 The ligand-field spectrum of MnO_4^{2-} in K_2CrO_4 at 4·2 K

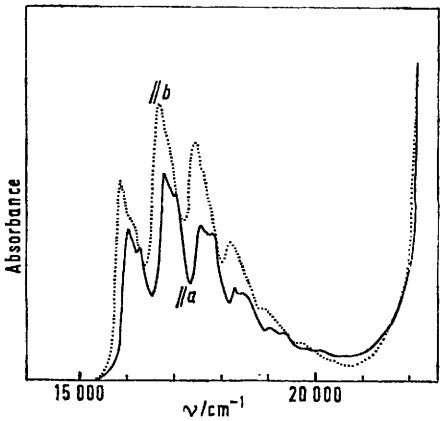

FIGURE 6 The charge-transfer spectrum of MnO_4^{2-} in K_2CrO_4 at 4·2 K

which we have not ourselves investigated. The far-infrared spectra of mulls [9] contain absorption peaks as follows: K_2SO_4, 59, 90, 170; Rb_2SO_4, 55, 88, 145; Cs_2SO_4, 58, 70, 90, 125 cm^{-1}. These correlate reasonably well with the excited state frequencies listed in Table 4. For example, in K_2SO_4

TABLE 4

Vibrational frequencies and band origins giving best fit to the ligand-field spectra of MnO_4^{2-} in various host lattices (cm^{-1})

	K_2SO_4		RB_2SO_4		Cs_2SO_4		K_2CrO_4	
	E // *a*	*E* // *b*	*E* // *a*	*E* // *b*	*E* // *b*	*E* // *a*	*E* // *b*	*E* // *b*
I	10 846	10 840	10 721	10 723	10 553	10 556	10 646	10 647
II	11 211	11 185	11 062	11 064	10 890	10 890	10 975	10 975
III	11 521	11 507	11 400	11 392	11 317	11 213	11 308	11 315
ν_L (1)	80		76		58		50	
ν_L (2)					106			
ν_L (3)	160		126		128		100	
ν_L (4)					206		190	
ν_4	321		314		298		310	
ν_1	795		783		679		774	

[8] C. Shantakumari, *Proc. Indian Acad. Sci.*, 1953, **37**, *A*, 393.

[9] R. A. Nyquist and R. O. Kegel, 'Infrared Spectra of Inorganic Compounds (3500—45 cm^{-1}),' Academic Press, London, 1971.

and Rb_2SO_4 the two highest-frequency ground-state vibrational modes each have their frequencies reduced by 5—10% in the excited state if we identify them with $\nu_L(1)$ and $\nu_L(3)$. In Cs_2SO_4, which has one extra lattice vibrational band both in the infrared and electronic spectra, it may be preferable to correlate $\nu_L(1)$ (58 cm^{-1}) in the latter with the infrared peak at 70 cm^{-1} rather than the one at 58 cm^{-1} since in K_2SO_4 and Rb_2SO_4 the lowest frequency bands in the infrared spectrum do not appear to correspond to any major sideband in the electronic spectrum.

On the other hand K_2CrO_4 has been the subject of a single-crystal Raman and infrared study,[10] in which the symmetries of a large number of the lattice modes were determined. The lowest frequency peaks found in the vibrational spectrum are at 58 cm^{-1} (B_{1g} and B_{1u}), and no doubt one or other of these correlates with the vibronic sideband at 50 cm^{-1}. The vibrational spectra contain a high density of peaks in the region 85—120 cm^{-1}, so it is difficult to decide which corresponds to the vibronic sideband peak at 100 cm^{-1}. For example, modes of even parity are reported [10] at 84 (A_{1g}), 87 (B_{1g}), 94 (B_{1g} and B_{3g}), 119 (B_{3g}), and 120 cm^{-1} (B_{2g}), while odd-parity modes are found at 104 (B_{3u}), 107 (B_{1u}), and 112 cm^{-1} (B_{2u}). In the vibrational spectrum there are further sets of modes of both parities grouped around 140 and 165 cm^{-1}, neither of which appears to give rise to any corresponding sidebands in the electronic spectrum. The sideband of highest frequency which may reasonably be assigned to a lattice mode is at 190 cm^{-1}, and no doubt correlates with one of four vibrational modes, 180 (B_{1u} and B_{3u}), 181 (A_{1g}), and 182 cm^{-1} (B_{3g}). In making these comparisons, of course, it is important to bear in mind that, because of the $\Delta k = 0$ selection rule for photons, the infrared and Raman results refer only to excitations at the centre of the Brillouin zone, whilst the electronic transition of a guest ion may be coupled to an entire branch of the host lattice phonon spectrum. It may well be that in some cases the critical point of the phonon density of states lies near the edge of the Brillouin zone. Depending on whether the phonon branch in question has a positive or negative dispersion, the frequency interval between the peak of the vibronic sideband and the electronic origin may then be greater or less than that of the corresponding peak in the infrared or Raman spectrum.

DISCUSSION

The Charge-transfer Bands.—In our previous paper on the manganate spectrum [1] we presented evidence for the assignment of the lowest-energy charge-transfer transition as $^2T_2$. This assignment is further confirmed by the extended series of results presented here. In Rb_2SO_4 and Cs_2SO_4 the two $^2A'$ and one $^2A''$ required from the decomposition of a $^2T_2$ state by a C_s site perturbation are at once identified with the origins labelled IA and IB in the $E \parallel b$ spectrum and IC in the $E \parallel a$ (Table 1). As mentioned above, in the K_2CrO_4 host lattice the second $^2A'$ component appears only as a shoulder on the first.

A number of interesting comparisons can be made between the spectra in the three sulphate lattices. With increasing radius of the alkali-metal cation all three components of the $^2T_2$ transition shift to lower energy, the $^2A''$ remaining always at higher energy than the two $^2A'$. However, the overall energy spread of the components decreases from the K to the Cs salt, almost entirely as a result of a decreasing interval between the two $^2A'$ components. Thus, we have

	K_2SO_4	Rb_2SO_4	Cs_2SO_4	
$^2A'' - {}^2A'$ (1)	68	64	72	cm^{-1}
$^2A'$ (1) $-$ $^2A'$ (2)	116	74	55	

The interval $^2A''$—$^2A'$ (1) is essentially constant, within the experimental error of the measurement. Unfortunately we have no information on the detailed bond length and angle changes from K_2SO_4 to Cs_2SO_4 and thus cannot make any further comment on this variation in the site-group perturbation.

Some features of the vibrational intervals in the sulphate hosts also deserve comment. As might be expected on increasing the unit-cell dimensions, and thus releasing compression on the guest ion in its excited state, the totally symmetric stretching mode of the MnO_4^{2-} decreases in frequency, although the trend in ν_4 is less obvious.

The existence of a well-resolved progression in ν_1 up to five quanta long makes it worthwhile to examine the Franck–Condon factors of the members, with a view to discovering the amount by which the molecule is expanded in the first charge-transfer excited state, and whether the expansion is affected by the host lattice. Assuming that the ground and excited-state potential-energy surfaces are harmonic, and that the vibration frequency is the same in the two states, the intensity of the $0 \longrightarrow n$ member of the progression, I_n, is

$$I_n = (k/n)I_{n-1}$$

where $k = 2\pi^2\nu\ cm\ (\Delta r)^2/h$, Δr being the change in bond length.[11] In Table 5 are listed the results of an analysis using this formula. The $E \parallel a$ spectrum is considered the more suitable for analysis since only one origin is observed, and the Franck–Condon factors are more easily estimated. Three points emerge from Table 5: first, that while it is possible to obtain a rough fit to the relative intensities in the progressions using average values of k, the observed and calculated intensities deviate significantly from one another. Secondly, if one calculates values of k to give agreement between observed and calculated intensities for each individual vibrational member, the values vary monotonically along the progressions in all three sulphate lattices. Finally, accepting average values of k as a rough approximation, these average k values increase monotonically from K_2SO_4 to Rb_2SO_4 to Cs_2SO_4.

Since successive vibrational quanta in the excited state show no clear trend towards smaller values, the variation of k along the vibrational progression cannot be attributed to anharmonicity. It is most likely the result of inclusion of sidebands due to excitation of non-totally symmetric modes within the same band envelopes, the contributions of which to the integrated band area of each

[10] D. M. Adams, M. A. Hooper, and M. H. Lloyd, *J. Chem. Soc.* (*A*), 1971, 946.
[11] C. J. Ballhausen, *Theoret. Chim. Acta*, 1963, **1**, 285.

member may vary along the progression if the Franck–Condon factors of, for example, the *e* mode differed from those of a_1. In his analysis of the Franck–Condon factors in the MnO_4^- spectrum Ballhausen [11] found reasonably constant values of *k* through five members ot a progression in ν_1. However, that spectrum shows better resolution of the individual members than in MnO_4^{2-}. If, in our case, we take the average values of *k* for the first few members of the progressions as representing approximate estimates of the expansion of the excited state with changing host lattice, it is clear that the expansion increases monotonically from the K to the Cs salt. This parallels the decrease in the ν_1 frequency in the excited

TABLE 5

Franck–Condon factors for the lowest-energy charge-transfer transition of MnO_4^{2-} in sulphate host lattices ($E \parallel a$)

	K_2SO_4			Rb_2SO_4			Cs_2SO_4		
	I_n/I_o			I_n/I_o			I_n/I_o		
		Calc.			Calc.			Calc.	
n	Obs.	(k = 1·35)	*k*	Obs.	(k = 1·45)	*k*	Obs.	(k = 1·55)	*k*
0	0·81	0·81	—	0·73	0·73	—	0·72	0·72	—
1	1·00	1·09	1·34	1·00	1·06	1·37	1·00	1·12	1·39
2	0·73	0·74	1·46	0·76	0·77	1·52	0·85	0·86	1·70
3	0·41	0·33	1·69	0·46	0·37	1·82	0·52	0·45	1·84
4	0·20	0·11	1·95	0·25	0·13	2·17	0·33	0·17	2·54
5	0·10	0·03	2·5	0·13	0·04	2·60	0·19	0·05	2·88

state and the energy of the zero-phonon lines. It is also of interest that the values of *k*, in so far as they have any precise meaning, are smaller than that found by Ballhausen [11] for the lowest $^1T_2$ charge transfer transition of MnO_4^- in $KClO_4$ (1·73). Since the excited state ν_1 vibrational frequencies of the two ions are quite similar, this corresponds to a smaller expansion of $^2T_2(t_1^5e^2)$ relative to $^2E(t_1^6e^1)$ than of $^1T_2(t_1^5e^1)$ relative to $^1A_1(t_1^6e^0)$.

The Ligand Field Band.—(a) *Electronic origin lines.* The main features of the electronic origin lines in all four host lattices may be summarised as follows.

(1) Three origins are observed, all of which are present in both the $E \parallel a$ and $E \parallel b$ spectra.

(2) In both $E \parallel a$ and $E \parallel b$ spectra the relative intensities of the three origins are very similar. That at lowest energy is much weaker than the other two, which have approximately equal intensity, *i.e.* $I_1 \ll I_2$, $I_2/I_3 \simeq 1$.

(3) All the bands in the $E \parallel b$ spectrum are more intense than those in the $E \parallel a$.

The third point has already been explained in our previous paper,[1] where it was pointed out that if one takes into account the orientations of the four SO_4^{2-} ions in the unit cell of A_2SO_4, which we assume to be randomly substituted by MnO_4^{2-}, and the effect of the lattice site-group perturbation, for a $^2E \longrightarrow {}^2T_2$ transition there are two alternative possibilities: either the ground state is $^2E_{x^2-y^2}$ and the $E \parallel b$ spectrum is more intense than $E \parallel a$, or the ground state is $^2E_{z^2}$ and $E \parallel a$ is more intense than $E \parallel b$. Since the first alternative is that observed, we have further evidence that in all four lattices the ground state is $^2E_{x^2-y^2}$, in agreement with the e.s.r. result for MnO_4^{2-} in K_2CrO_4.[12]

On the other hand, if one considers only the site-group perturbation the first two experimental points cannot be explained. Thus, if the ground state were correctly classified as $^2A''$, and the $^2T_2$ excited state was decomposed by the C_s site perturbation into one $^2A''$ and two $^2A'$, we should expect to find two electronic origins in the $E \parallel b$ spectrum and only one in the $E \parallel a$, just as we found, in fact, for the first charge-transfer transition. It appears that in the ligand field (though apparently not in the charge transfer) $^2T_2$ state, spin–orbit coupling must also be considered. One might also note that formally, the $^2T_2$ parent state is susceptible to Jahn–Teller distortion, which may compete with, or add to, the static site-group distortion and have some influence on the polarisation mixing observed. On the other hand, since the lattice-induced distortion is inevitably present, any Jahn–Teller effect would necessarily be of second-order type. Furthermore, at least if the Jahn–Teller active mode were *e*, the basis functions *xy*, *xz*, *yz* of a T_2 state remain diagonal, so no mixing of polarisations would be expected.[13] For these reasons we first seek an explanation for the polarisation mixing in spin–orbit coupling rather than the Jahn–Teller effect.

To take spin-orbit coupling into account, we must examine MnO_4^{2-} in the double group C_s*. With the axis orientation of Figure 7, where σ denotes the mirror plane, the ground state $^2E_{x^2-y^2}$ can be either

$$\Gamma_3 : e^-_{x^2-y^2} \quad \text{or} \quad \Gamma_4 : e^+_{x^2-y^2} \qquad (1)$$

The $^2T_2$ excited states in the C_s* group can be classified as follows:

$$\Gamma_3 : t_{2z}{}^+;\ (1/\sqrt{2})(t_{2x}{}^+ + t_{2y}{}^+);\ (1/\sqrt{2})(t_{2x}{}^- - t_{2y}{}^-) \qquad (2)$$
$$\Gamma_4 : t_{2z}{}^-;\ (1/\sqrt{2})(t_{2x}{}^- + t_{2y}{}^-);\ (1/\sqrt{2})(t_{2x}{}^+ - t_{2y}{}^+)$$

where $t_{2z}{}^+$ *etc.* is the spin-orbital of the unpaired electron and *e*, t_2 are *d*-type molecular orbitals. A first-order

[12] A. Carrington, D. J. E. Ingram, K. A. K. Lott, D. Schonland, and M. C. R. Symons, *Proc. Roy. Soc.*, 1960, *A*, **254**, 101; D. Schonland, *Proc. Roy. Soc.*, 1960, *A*, **254**, 111.

[13] M. D. Sturge, 'Solid State Physics,' ed. F. Seitz and D. Turnbull, 1967, **20**, 98.

perturbation will the mix together the functions within each irreducible representation.

Since the electric-dipole transition-moment operators along the crystallographic axes μ_a, μ_c, and μ_b belong to the irreducible representations Γ_1 and Γ_2 respectively, transitions are allowed as follows:

$$\begin{aligned} E \,//\, a, E \,//\, c &: \Gamma_3 \longrightarrow \Gamma_3;\ \Gamma_4 \longrightarrow \Gamma_4 \\ E \,//\, b &: \Gamma_3 \longrightarrow \Gamma_4;\ \Gamma_4 \longrightarrow \Gamma_3 \end{aligned} \qquad (3)$$

From these selection rules, and the orbital compositions of equations (1) and (2) it is now clear that as a result of spin–orbit coupling three origins may be observed in both polarisations.

The spin–orbit coupling Hamiltonian can be written as:

$$H'' = \xi . \mathbf{l} . \mathbf{s} = \xi(\mathbf{l}_{z'} . \mathbf{s}_{z'} + \tfrac{1}{2}\mathbf{l}_+ . \mathbf{s}_- + \tfrac{1}{2}\mathbf{l}_- \mathbf{s}_+) \qquad (4)$$

If, in the C_s* point group, we call the axis orthogonal to the mirror plane z', then the $\mathbf{l}_{z'}$ and $\mathbf{s}_{z'}$ operators belong to the irreducible representation Γ_1, and $\mathbf{l}_+$, $\mathbf{l}_-$, $\mathbf{s}_+$, $\mathbf{s}_-$ to the irreducible representation Γ_2. To apply equation (4), we approximate the e and t_2 molecular orbitals as d-atomic orbitals, referring them to the x', y', z' axis system of Figure 7. Thus we have

$$\begin{aligned} e_{z^2} &\simeq d_{z^2} = -\frac{\sqrt{3}}{2} d_{x'^2-y'^2} - \frac{1}{2} d_{z'^2} \\ e_{x^2-y^2} &\simeq d_{x^2-y^2} = d_{x'z'} \\ t_{2z} &\simeq d_{xy} = \frac{1}{2} d_{x'^2-y'^2} - \frac{\sqrt{3}}{2} d_{z'^2} \end{aligned} \qquad (5)$$

$$\frac{1}{\sqrt{2}}(t_{2x} + t_{2y}) \simeq \frac{1}{\sqrt{2}}(d_{zy} + d_{xz}) = d_{x'y}$$

$$\frac{1}{\sqrt{2}}(t_{2x} - t_{2y}) \simeq \frac{1}{\sqrt{2}}(d_{zy} - d_{xz}) = -d_{y''z}$$

We can then write the first order perturbation matrix including both the distortion and spin-orbit coupling as follows:

$$\begin{vmatrix} A - E & \frac{1}{2}i\xi + D & -\frac{1}{2}i\xi \\ -\frac{1}{2}i\xi + D & B - E & -\frac{1}{2}\xi \\ \frac{1}{2}i\xi & -\frac{1}{2}\xi & C - E \end{vmatrix} = 0 \qquad (6)$$

where:

$$A = \langle t_{2z} \,|\, H' \,|\, t_{2z} \rangle$$

$$B = \left\langle \frac{1}{\sqrt{2}}(t_{2x} + t_{2y}) | H' | \frac{1}{\sqrt{2}}(t_{2x} + t_{2y}) \right\rangle$$

$$C = \left\langle \frac{1}{\sqrt{2}}(t_{2x} - t_{2y}) | H' | \frac{1}{\sqrt{2}}(t_{2x} - t_{2y}) \right\rangle$$

$$D = \left\langle \frac{1}{\sqrt{2}}(t_{2x} + t_{2y}) | H' | t_{2z} \right\rangle$$

H' = perturbation Hamiltonian for the lattice site-group symmetry

ξ = spin-orbit coupling constant

In fact there exist two identical matrices [equation (6)], one for Γ_3 and one for Γ_4. Then the two degenerate wave functions for each excited state with energy E_r are:

$$\begin{aligned} \psi_r(\Gamma_3) = a_r t_{2z}^{+} + b_r \frac{1}{\sqrt{2}}(t_{2x}^{+} + t_{2y}^{+}) + \\ c_r \frac{1}{\sqrt{2}}(t_{2x}^{-} - t_{2y}^{-}) \end{aligned} \qquad (7)$$

$$\begin{aligned} \psi_r(\Gamma_4) = a_r t_{2z}^{-} + b_r \frac{1}{\sqrt{2}}(t_{2x}^{-} + t_{2y}^{-}) + \\ c_r \frac{1}{\sqrt{2}}(t_{2x}^{+} - t_{2y}^{+}) \end{aligned}$$

If we express the transition moment operators along the crystallographic axes in terms of those along the x, y, z axes of Figure 7 and we take into account the T_d symmetry of the t_2 MO, the transition-moment integrals become:

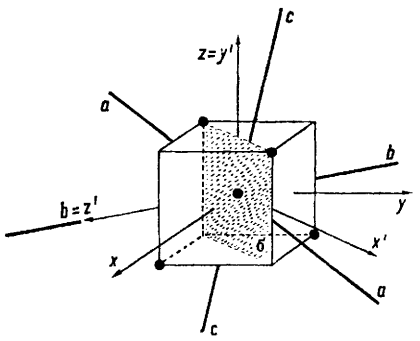

FIGURE 7 The orientation of the molecular and crystal axes of MnO_4^{2-} in the alkali-metal sulphate host lattices

$$\begin{aligned} \langle e_{x^2-y^2}^{-} |\mu_a|\, \psi_r(\Gamma_3)\rangle \\ = \langle e_{x^2-y^2}^{+} |\mu_a| \psi r(\Gamma_4)\rangle = -c_r \cos\theta \,.\, T \\ \langle e_{x^2-y^2}^{+} |\mu_b| \psi_r(\Gamma_3)\rangle \\ = \langle e_{x^2-y^2}^{-} |\mu_b| \psi_r(\Gamma_4)\rangle = b_r T \\ \langle e_{x^2-y^2}^{-} |\mu_o| \psi_r(\Gamma_3)\rangle \\ = \langle e_{x^2-y^2}^{+} |\mu_o| \psi_r(\Gamma_4)\rangle = c_r \sin\theta \,.\, T \end{aligned} \qquad (8)$$

where $T = \langle e_{x^2-y^2} | \mu_x | t_{2x} \rangle$ and $\theta\,(\simeq 35°)$ is the angle between the axes a and z. Since all four inequivalent sulphate groups in the unit cell (which are assumed randomly substituted by MnO_4^{2-}) have the same values of $\cos^2\theta \simeq 2/3$ and $\sin^2\theta \simeq 1/3$, the ratios of the intensities of the three origins must be

$$\begin{aligned} E \,//\, a, E \,//\, c \quad & I_1 : I_2 : I_3 = |c_1|^2 : |c_2|^2 : |c_3|^2 \\ E \,//\, b \quad & I_1 : I_2 : I_3 = |b_1|^2 : |b_2|^2 : |b_3|^2 \end{aligned} \qquad (9)$$

We now wish to discover whether it is possible to find values of the distortion parameters A, B, C, D and the spin-orbit coupling constant ξ of equation (6), which reproduce the observed frequency intervals between the

band origins, while at the same time fitting the relative intensities. The latter correspond to

$$|c_1|^2 \ll |c_2|^2,\ |b_1|^2 \ll |b_2|^2$$

and

$$|c_2|^2 \sim |c_3|^2,\ |b_2|^2 \sim |b_3|^2.$$

Our prccedure is as follows: for given values of ξ and D, we calculate the values of the parameters A, B, C which reproduce the observed energy differences between the three origins in each lattice. Then with these parameters we calculate the coefficients a_r, b_r, c_r for each of the energies E_r, and hence obtain the intensities. In this way one finds that the theoretical intensity ratios are very sensitive to variations in ξ, but very little to those in D. Because the parameters A, B, C, D, and ξ must have real values, the form of equation (6) requires that ξ cannot have a larger value than that ($\xi_{max.}$) for which $(p/3)^3 = (q/2)^2$, where $p = -(E_1E_2 + E_1E_3 + E_2E_3) - 3/4\xi^2$ and $q = -E_1E_2E_3 - 1/4\xi^3$. For larger values of ξ than $\xi_{max.}$ there are no real values of A, B, C, which reproduce the energies E_1, E_2, E_3 ($E_1 + E_2 + E_3 = 0$). In particular when $B = C$ and $D = 0$, ξ is equal to $\xi_{max.}$.

Table 6 lists the results obtained for K_2SO_4 for several different values of ξ and D (quite comparable results were obtained for the other three lattices). From this Table we see that the best agreement with the experimental intensity ratios is obtained when ξ has its maximum value and $D = 0$. This means that the lattice site-group pertubation has stabilised t_{2z} with respect to $\frac{1}{\sqrt{2}}(t_{2x} + t_{2y})$ and $\frac{1}{\sqrt{2}}(t_{2x} - t_{2y})$ and that the latter are almost degenerate ($-\frac{1}{2}A = B = C$). In addition it means that

$$\begin{aligned} &\langle t_{2x}|H'|t_{2y}\rangle \ll \langle t_{2x}|H'|t_{2x}\rangle + \langle t_{2y}|H'|t_{2y}\rangle \\ &\left\langle \frac{1}{\sqrt{2}}(t_{2x} + t_{2y})|H'|t_{2z}\right\rangle \ll \\ &\left\langle \frac{1}{\sqrt{2}}(t_{2x} + t_{2y})|H'|\frac{1}{\sqrt{2}}(t_{2x} + t_{2y})\right\rangle - \langle t_{2z}|H'|t_{2z}\rangle \end{aligned} \qquad (10)$$

TABLE 6

Calculation of the intensities and separations of the low-symmetry components of the ligand-field $^2T_2$ state of MnO_4^{2-} in K_2SO_4

ξ	D	A	B	C	$\lvert c_1\rvert^2$	$\lvert c_2\rvert^2$	$\lvert c_3\rvert^2$	$\lvert b_1\rvert^2$	$\lvert b_2\rvert^2$	$\lvert b_3\rvert^2$
264·6	0	−280	140	140	0·043	0·500	0·457	0·043	0·500	0·457
	50	−274	134	140	0·043	0·500	0·457	0·055	0·487	0·458
	100	−255	115	140	0·043	0·500	0·457	0·094	0·465	0·441
254·6	0	−283	191	92	0·054	0·627	0·319	0·030	0·366	0·604
		−283	92	191	0·030	0·366	0·604	0·054	0·627	0·319
	50	−278	186	92	0·054	0·627	0·319	0·040	0·362	0·598
		−276	85	191	0·030	0·366	0·604	0·069	0·616	0·314
	100	−261	169	92	0·054	0·627	0·319	0·072	0·349	0·579
		−254	63	191	0·030	0·366	0·604	0·120	0·579	0·300

Table 6 lists the results obtained for K_2SO_4 for several different values of ξ and D (quite comparable results were obtained for the other three lattices). From this Table we see that the best agreement with the experimental intensity ratios is obtained when ξ has its maximum value and $D = 0$. This means that the lattice site-group pertubation has stabilised t_{2z} with respect to $\frac{1}{\sqrt{2}}(t_{2x} + t_{2y})$ and $\frac{1}{\sqrt{2}}(t_{2x} - t_{2y})$ and that the latter are almost degenerate ($-\frac{1}{2}A = B = C$). In addition it means that

which holds when the lattice-site group pertubation of symmetry C_s differs very little from that of higher symmetry D_{2d}. This agrees with the fact that the SO_4^{2-} ions in K_2SO_4 indeed have a symmetry rather close to D_{2d}.[14] Although the five disposable parameters of equation (6) cannot be fitted with complete accuracy to the experimental data, it is nevertheless clear that spin–orbit coupling is indeed the mechanism responsible for mixing the polarisations of the three origin lines of the ligand-field $^2T_2$ state in this C_s site. It is worth noting, however, that the parameters A, B, C, D may be considered equally as representing a static site-group perturbation or a Jahn–Teller distortion. Thus, if our T_2 state couples with a vibrational mode transforming as ε the perturbation matrix elements are:[15]

$$\begin{aligned} A &= \langle t_{2z}|H'|t_{2z}\rangle = c_\varepsilon S_{2a} \\ B &= \left\langle \frac{1}{\sqrt{2}}(t_{2x} + t_{2y})|H'|\frac{1}{\sqrt{2}}\ (t_{2x} + t_{2y})\right\rangle = -\frac{1}{2}c_\varepsilon S_{2a} \\ C &= \left\langle \frac{1}{\sqrt{2}}(t_{2x} - t_{2y})|H'|\frac{1}{\sqrt{2}}(t_{2x} - t_{2y})\right\rangle = -\frac{1}{2}c_\varepsilon S_{2a} \\ D &= \left\langle \frac{1}{\sqrt{2}}(t_{2x} + t_{2y})|H'|t_{2z}\right\rangle = 0 \qquad (11) \\ &\left\langle \frac{1}{\sqrt{2}}(t_{2x} + t_{2y})|H'|\frac{1}{\sqrt{2}}(t_{2x} - t_{2y})\right\rangle = \frac{\sqrt{3}}{2}c_\varepsilon S_{2b} \end{aligned}$$

where S_{2a} and S_{2b} are symmetry co-ordinates. By defining the two polar co-ordinates r and ϕ by

$$S_{2a} = r\cos\phi \qquad S_{2b} = r\sin\phi$$

for the potential surface in S_{2a}, S_{2b} space we have

$$E = \frac{1}{2}kr^2 - c_\varepsilon r\cos\phi.$$

Minimising E with respect to r and ϕ, we have

$$\phi = 0 \qquad r = c_\varepsilon/k$$

which corresponds to $S_{2a} = c_\varepsilon/k$, $S_{2b} = 0$ and hence

$$-\frac{1}{2}A = B = C \qquad D = 0$$

[14] R. G. Wyckoff, 'Crystal Structures,' John Wiley and Sons, New York, 1966.

[15] C. J. Ballhausen, 'Introduction to Ligand Field Theory,' McGraw-Hill, New York, 1963, p. 213.

a situation which corresponds very closely to the parameters which we have found.

Since the analysis yields a direct estimate of the effective spin–orbit coupling constant of the $^2T_2$ state, it is worth considering briefly the significance of the parameters extracted.

As a result of using different methods for fitting the atomic spectra, different authors [16–18] have given rather discordant estimates of the one-electron spin–orbit coupling constants of Mn as a function of ionic charges of +1 and +2. For example,

	Ref. 16	Ref. 17	Ref. 18	
Mn^+	224	254	255	cm^{-1}
Mn^{2+}	335	347	300	

Strictly speaking, the effective spin–orbit coupling constant for the $^2T_2$ state of MnO_4^{2-} is that of a single electron in the t_2 d-type molecular orbital:

$\langle \frac{1}{2}t_2 \| s \cdot u \| \frac{1}{2}t_2 \rangle$, where $u = \Sigma_i \xi_i l_i$, the summation being extended over all atomic centres in the molecule. In fact, for a tetrahedral molecule [19] ML_4

$$\langle \tfrac{1}{2}t_2 \| s \cdot u \| \tfrac{1}{2}t_2 \rangle = [C^2_{4p\mathrm{M}}\xi_{4p\mathrm{M}} - C^2_{3d\mathrm{M}}\xi_{3d\mathrm{M}} - (\sqrt{2}C_{p\delta\mathrm{L}}C_{p\pi\mathrm{L}} - \tfrac{1}{2}C^2_{p\pi\mathrm{L}})\xi_{p\mathrm{L}}] \quad (12)$$

Apart from variations in $\xi_{3d\mathrm{M}}$ due to the screening of the electron by other electrons on the same centre (Jørgensen's [20] ' central field covalency ') the observed value of this matrix element depends on the magnitudes of the Mn and O molecular orbital coefficients (' symmetry restricted covalency ' [20]). Since the atomic spin-orbital coupling constant of O is negligible compared with that of Mn, equation (7) becomes approximately

$$\langle \tfrac{1}{2}t_2 \| s \cdot u \| \tfrac{1}{2}t_2 \rangle \sim C^2_{3d\mathrm{M}}\xi_{3d\mathrm{M}} \quad (13)$$

Unfortunately equation (11) still contains two parameters and from our experiments we have only a single observable, the effective spin–orbit coupling constant. Thus we cannot carry the analysis any further except to say that, since the upper limit of $C_{3d\mathrm{M}}{}^2$ is close to one (or, indeed, equal to one if we neglect overlap) the lower limit of the charge on the Mn must be $+1{\cdot}3 \pm 0{\cdot}1$. To arrive at this estimate we have used the average value of ξ fitting the MnO_4^{2-} spectrum, and have also taken a simple average between the available estimates of ξ from the atomic spectra. The formal upper limit of the charge on Mn is clearly +6 (*i.e.* equal to the oxidation state). Since the value of ξ corresponding to this charge is 540 cm^{-1} (ref. 18) we arrive at an estimate for the lower limit of $C_{3d\mathrm{M}}$ of *ca.* 0·7.

A further point which can now be explained by considering the role of spin–orbit coupling concerns the polarisation behaviour of the three low-symmetry components of the charge transfer $^2T_2$ state. As we have already mentioned, this state is decomposed by the C_s site perturbation into two $^2A'$ and one $^2A''$, whose polarisations unlike those of the ligand-field $^2T_2$, remain quite unmixed. We can now see that this behaviour is a result of a greatly reduced effective spin–orbit coupling constant compared with the ligand-field $^2T_2$. According to the analysis in our previous paper [1] the lowest charge-transfer $^2T_2$ term comes from the $t_1^5(^2T_1)e^2(^3A_2)$ configuration, the orbital angular momentum of which resides in the completely non-bonding t_1, confined entirely to the O 2p orbitals. Because the one-electron spin–orbit coupling constant of O is much smaller than that of Mn the first-order descriptions of the three low-symmetry components of the charge-transfer transition remain valid, and their polarisations are pure.

(b) *Vibronic sidebands.* Figures 1, 3, and 5 show that underlying the sharp-line structure in each of the host lattices is a broad and rising continuum of absorption, which makes it impossible to perform an analysis of the Franck–Condon factors within the vibrational progressions of the type which we carried out on the first charge-transfer transition. All that can be said, qualitatively, is that it appears as if the origin line is the most intense in each vibronic progression, as one would expect if the excited state were not much expanded relative to the ground state. On average, the ν_1 and ν_4 frequencies in the ligand-field excited state are also slightly higher than those in the first charge-transfer state, although the difference is not very great. The most interesting vibronic feature of the ligand-field transition however, is the appearance of quite well resolved structure due to lattice vibrational modes. Unfortunately, however, no lattice phonon spectra for Cs_2SO_4 appear ever to have been reported.

Energy Shifts of the Transitions.—The set of host lattices used in this work offers a good opportunity for comparing the relative shifts of ligand-field and charge-transfer transitions as the Madelung potential around the MnO_4^{2-} is varied. In fact the baricentres of both transitions shift towards lower frequency with increasing atomic number of the alkali-metal cation, the ligand-field transition shifting slightly more than the charge transfer. Since the former results from an excitation from $e \longrightarrow t_2$ and the latter from $t_1 \longrightarrow e$, one must conclude that both energy separations are diminishing, and that there is no exclusive sensitivity of the t_1 orbital to changing cation, although this orbital is confined to the outer part of the molecule. Perhaps the most plausible model is that on decreasing the Madelung potential around the MnO_4^{2-}, the binding energy of all the orbitals diminishes. In agreement with this is the fact that the ν_1 frequencies in both types of excited state diminish as the cation size increases. A similar observation was made many years ago by Teltow [21] with regard to MnO_4^- in a series of

[16] D. S. McClure, ' Spectra of Molecules and Ions in Crystals,' Academic Press, London, 1959, p. 78.
[17] J. S. Griffith, ' Theory of Transition Metal Ions,' Cambridge University Press, 1961, p. 487.
[18] B. N. Figgis, ' Introduction to Ligand Fields,' Interscience, London, 1966, p. 60.
[19] B. D. Bird and P. Day, *J. Chem. Phys.*, 1968, **49**, 392.
[20] C. K. Jørgensen, ' Absorption Spectra and Chemical Bonding, in Complexes,' Pergamon Press, Oxford, 1962.
[21] J. Tetlow, *Z. phys. Chem.*, 1939, *B***40**, 397.

alkali-metal perchlorate crystals. However, he found that both in the perchlorate lattices and in a similar series of pure permangate salts, the lowest frequency $^1T_2$ state actually shifts to the blue with increasing cation size. Why MnO_4^- and MnO_4^{2-} should behave in the reverse fashion in this respect is not clear to us.

The behaviour of the chromate host lattice compared with the sulphates is also of interest. Relative to K_2SO_4 the MnO_4^{2-} ligand-field band in K_2CrO_4 is slightly red-shifted (217 cm^{-1} for the baricentre of the transition) while the charge-transfer band is red-shifted by 267 cm^{-1}. The position of the ligand-field baricentre in the K_2CrO_4 host is roughly half-way between that in Rb_2SO_4 and Cs_2SO_4, but the charge-transfer band lies to the red of that in Cs_2SO_4. At 16 000 cm^{-1}, the first charge-transfer band of MnO_4^{2-}, however, lies only 10 000 cm^{-1} lower than the first allowed charge-transfer transition of the chromate host lattice, so it is quite conceivable that the MnO_4^{2-} band is appreciably red-shifted by a second-order Davydov interaction with CrO_4^{2-} excitations.

We are grateful to N.A.T.O. for financial assistance and the S.R.C. for an equipment grant. The work in Parma is also partially supported by the C.N.R.

[3/406 *Received*, 21*st February*, 1973]